Available online at www.sciencedirect.com
ScienceDirect
Applied Surface Science 253 (2006) 1143–1149
applied surface science
www.elsevier.com/locate/apsusc

Elaboration of (1 1 1)-oriented La-doped PZT thin films on platinized silicon substrates

G. Leclerc [a,*], B. Domengès [b], G. Poullain [a], R. Bouregba [a]

[a] Laboratoire CRISMAT/CNRT, CNRS UMR 6508, Boulevard du Maréchal Juin, 14050 CAEN Cedex, France
[b] LAMIP, Laboratoire de microélectronique ENSICAEN-PHILIPS semiconductors, 2, rue de la Girafe, BP5120, F-14079 CAEN CEDEX 5, France

Received 24 December 2005; accepted 23 January 2006
Available online 13 March 2006

Abstract

PLZT thin films with different thickness were deposited in situ on platinum coated silicon substrates using a multi-target sputtering system. The purpose was to grow (1 1 1)-textured PLZT films on Pt (1 1 1). To this aim, the role of some key parameters on both crystalline quality and electrical properties was investigated. An ultra-thin TiO_2 seeding layer was deposited, prior to PLZT, which strongly affected the crystallographic orientation of the films. The relation between temperature deposition and film crystallinity is analysed. TEM observations show the presence of some very small grains of $Zr_{0.9}La_{0.1}O_{1.95}$ at the film bottom interface. In the range of thickness investigated, the plot of the inverse capacitance as a function of the film thickness split up into two different curves, each with a linear shape, which however allows determination of a single value of interface capacitance. Above a thickness of 400–500 nm a saturation of the dielectric properties seems to be reached.
© 2006 Elsevier B.V. All rights reserved.

PACS: 68.37.-d; 68.55.Jk; 77.84.-s; 81.15.Cd

Keywords: PLZT films; Ferroelectric; Multi-target sputtering; Interfaces; Electron microscopy

1. Introduction

Ferroelectric materials have retained much attention because they are good candidates for non-volatile RAM applications and they could be used in a wide variety of devices in thin film form [1–2]. PZT is known as one of the best ferroelectric materials with high dielectric properties. One way to still enhance the dielectric properties of PZT for DRAM applications consists to perform cationic substitution [3–4]. Lanthanum is considered as a doping element in PZT structure as it replaces Pb^{2+} in A-sites with a higher valence degree leading to the formula $Pb_{1-3y/2}La_yZr_xTi_{1-x}O_3$. Addition of higher valence impurities lowers the ferroelectric properties but tends to increase the dielectric response. In addition, PLZT has been shown to be less prone to the classical failures encountered in PZT [5], like fatigue and imprint [1].

Derived materials such as (Pb, La) (Zr, Ti)O_3 (PLZT) are also attractive because the modulation of the ferroelectric properties may be achieved by changing the amount of La dopant or by varying the Zr/Ti ratio [6–8]. To this aim, RF multi-target sputtering is particularly convenient because the amount of each cationic element can be monitored individually. To achieve potential devices like DRAM capacitor, industrial standard substrates like Si/SiO_2 and low temperature process are required. This may be obtained by in situ sputtering with substrate temperature around 500 °C.

The purpose of this paper is to describe the preparation of (1 1 1)-textured PLZT films by sputtering on platinum coated silicon substrates. The influence of the thickness of the films on the ferroelectric properties will also be considered, and the value of the interface capacitance resulting from ferroelectric layer/electrode interfaces will be determined.

2. Experimental procedure

PLZT thin films were prepared by RF sputtering using magnetron cathodes. Metallic targets (Pb, Zr and Ti) of 4 in.

* Corresponding author. Tel.: +33 2 31 45 29 11; fax: +33 2 31 95 16 00.
E-mail address: gerald.leclerc@ensicaen.fr (G. Leclerc).

0169-4332/$ – see front matter © 2006 Elsevier B.V. All rights reserved.
doi:10.1016/j.apsusc.2006.01.048

were used except for lanthanum ($La_2Ti_2O_6$ target) because of instability in air of this element. Pt(1 1 1)/TiO_2/SiO_2/Si substrates were heated (425–580 °C) during the deposition of PLZT thin films in order to achieve in situ crystallization. Platinum bottom electrodes were elaborated by sputtering and showed (1 1 1)-preferred orientation. Ferroelectric capacitors with 250 μm × 250 μm top electrodes were patterned by lift-off after sputtering platinum on the surface of the films. The crystalline structure of the films was examined with an X-ray Seifert diffractometer. The thickness was measured with a DEKTAK profilometer. Electron transparent lamella was Fib prepared in a FEI 200Xp using lift-off in situ technique [9]. TEM study was performed on a Jeol 2011 FEG-STEM equipped with a tilting rotating holder, a high resolution objective lens (d_{min} = 2.2 Å) and EDAX energy dispersive X-ray analyzer. For EDX line profiles, the electron nanobeam (1nm theoretical diameter) was kept 10 s at each analysis point for X-ray counting. Hysteresis measurements were performed by using the Sawyer-Tower circuit. A Hewlett-Packard 4294A LCR meter allowed the study of the dielectric response in the 100 Hz–1 MHz frequency range, the amplitude of the AC small signal was 5 mV.

In this study we focus on the mechanisms and the crucial steps of the crystallisation of (1 1 1)-oriented $Pb_{1-3y/2}La_yZr_xTi_{1-x}O_3$ thin films. To avoid coexistence of different phases we chose a composition in the tetragonal phase $Pb_{0.85}La_{0.1}Zr_{0.4}Ti_{0.6}O_3$ (named 10/40/60), which is far from any phase transition. Based on previous works [10–11], we used a seeding layer of TiO_2 deposited on the Pt bottom electrode prior to PLZT deposition. This layer promotes the crystallisation of the perovskite phase and allows the control of the growth axis. Under some special conditions, the use of an oxidizing titanium thin layer on Pt(1 1 1)/TiO_2/SiO_2/Si substrates leads to the (1 1 1) preferential orientation of the PLZT.

3. Results

3.1. Film crystallization

Heating treatment during PLZT deposition was investigated to determine the optimum growth temperature. During this study, the thickness of TiO_2 thin buffer layer was about 2–3 nm and that of PLZT films of around 150 nm. Fig. 1 shows the XRD pattern of PLZT 10/40/60 films grown at different temperatures. For temperatures below 450 °C, the films are amorphous even if a small pyrochlore phase line at 29° is present on the XRD pattern. At higher temperatures, the films crystallized in a single perovskite phase with (1 1 1)-preferential orientation. Considering that the (1 1 1) plane has the lowest surface energy and that the lattice mismatch with the (1 1 1) plane of platinum is about 2.5%, this may explain why the films orientation followed the Pt growth axis, even if a competition between ⟨1 1 1⟩ and ⟨1 0 1⟩ orientations was clearly visible on the XRD patterns. When the growth temperature was increased up to 580 °C, the XRD patterns revealed some degradation of the crystallization. Above this temperature the loss of lead species probably became substantial, leading to a decrease of the number of nucleation sites, and finally less crystallized films were obtained.

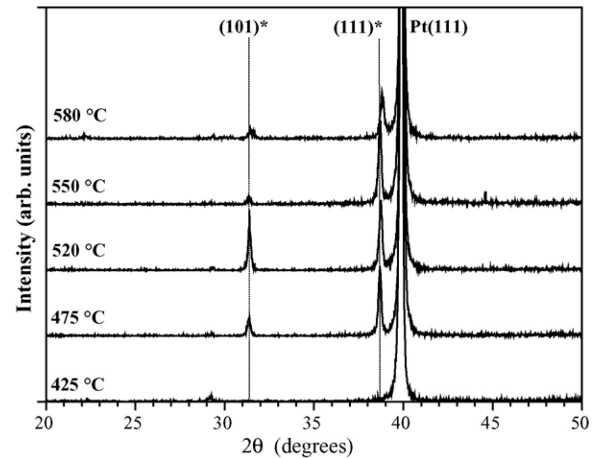

Fig. 1. XRD pattern of PLZT films crystallized in situ at different temperatures. The (*h k l*)* indexes are related to the perovskite phase.

Fig. 2 shows the evolution of the diffraction patterns with the thickness of the ultra-thin TiO_2 layer. The thickness is quoted as time of deposition. When the PLZT films were deposited without any TiO_2 layer, poor crystalline structure with random orientation was obtained. The presence of the titanium oxide seeding layer clearly promoted the crystallization of the (1 1 1) oriented PLZT perovskite. The diffraction patterns did not change significantly after further increase of the deposition time. Nevertheless, ferroelectric measurements revealed a large increase of leakage current for deposition time of TiO_2 larger than 6 min (see Fig. 3). This is consistent with the assumption that the TiO_2 seeding layer must cover sufficiently the platinum electrode to promote the nucleation [12], but however, the thickness of this TiO_2 seeding layer should also be minimised in order to avoid the formation of a detrimental interface layer. A study by AES depth profile of a sample with 3 min TiO_2 deposition time (Fig. 4) shows a well homogeneous composition within the film with only a very slight excess of Ti close to the interface. On the contrary, increase of the TiO_2 deposition

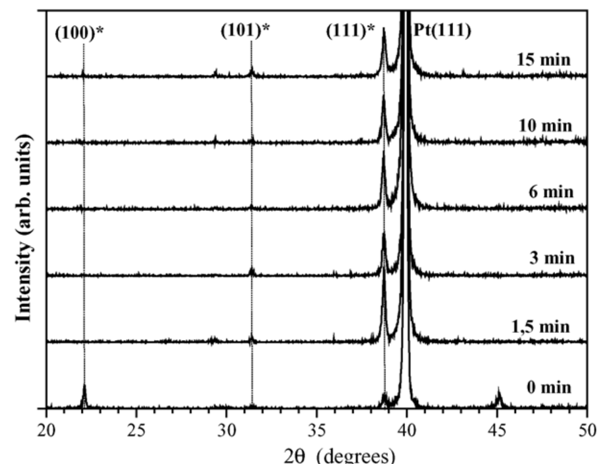

Fig. 2. XRD patterns of PLZT films with different thickness of the TiO_2 buffer layer. All films were grown at 550 °C.

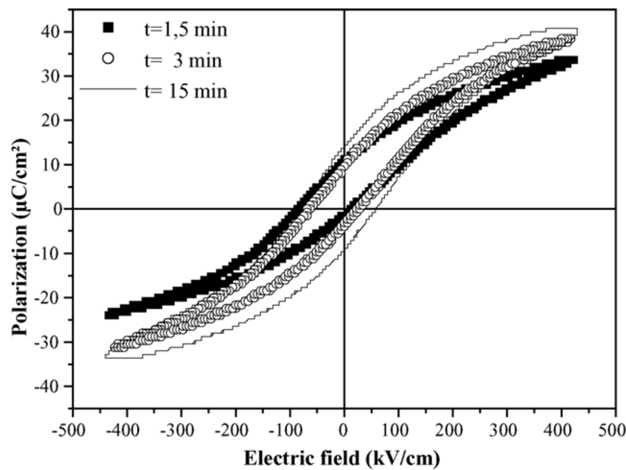

Fig. 3. Effect of the thickness of the TiO_2 seed layer on the hysteresis loops.

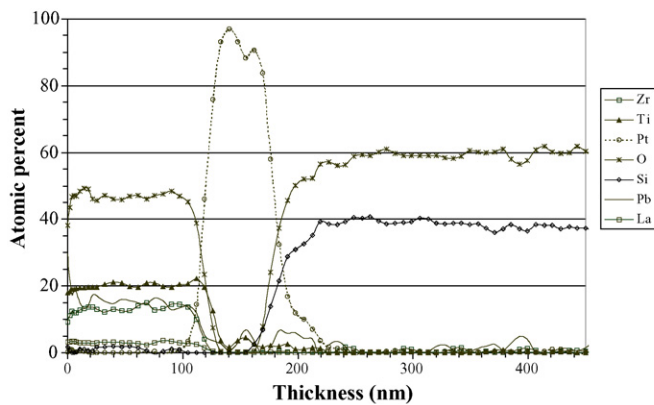

Fig. 4. AES depth profile for the sample with 3 min TiO_2 buffer layer deposition time.

time reveals an excess of titanium amount at the interface (not shown in the paper). This may contribute to formation of an interface layer detrimental to the ferroelectric properties of the Pt/PLZT/Pt capacitors as evidenced in Fig. 3.

Several works have been carried out concerning the role of an ultra-thin TiO_2 layer [11–20]. Different seeding layers like $PbTiO_3$ were also employed by other researchers [12,16,17]. Obviously the TiO_2 seeding layer promotes nucleation sites for

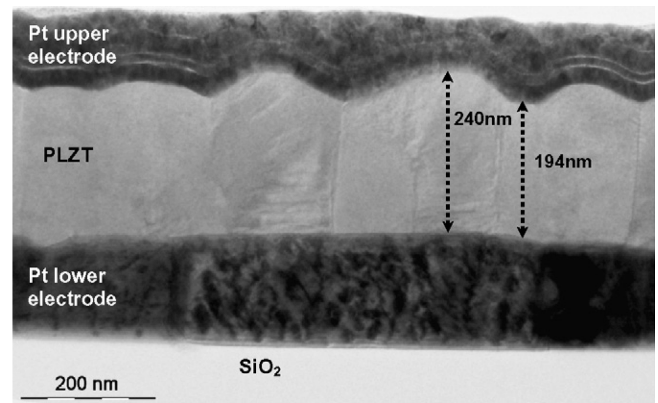

Fig. 5. Cross-sectional Medium resolution TEM analysis image of 240 nm thick (1 1 1)-oriented PLZT film with 3 min TiO_2 deposition time.

crystallization of PZT perovskite on platinum electrode. On one hand, the Ti rich PZT compounds have a lower activation energy [11,20]. Thus, during the first stage of the film growth, the Pb probably incorporates more easily through the reaction (1), minimizing the Lead deficiency (by evaporation) at the interface, hence preventing crystallization of pyrochlore phases.

$$TiO_2 + PbO \rightarrow PbTiO_3 \quad (1)$$

Then zirconium and lanthanum are likely to gradually incorporate during the subsequent growth of the film.

On the other hand, the good lattice matching between the Pt electrode and the perovskite film limits the interface strain. However, the possible gradual incorporation of elements at the first stage of the deposition suggests the existence of a continuous transition between the substrate and the film.

A cross-sectional TEM observation of a 240 nm thick (1 1 1)-oriented sample with 3 min TiO_2 layer deposition time (Fig. 5) was performed. The columnar structure of the film is clearly visible and its thickness varies from 190 nm to 240 nm. The observed columnar structure suggests that kinetics process was predominant. Indeed, as it was described in the Stranski-Krastanov diagram [21], columnar structure is often obtained when films are grown by sputtering.

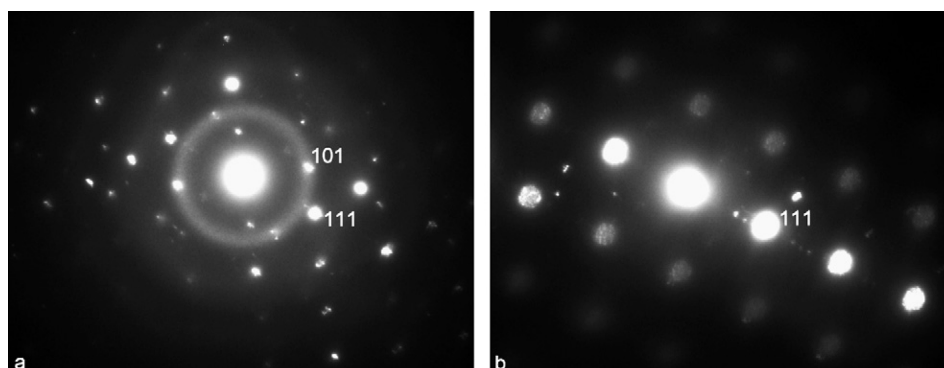

Fig. 6. Electron micro-diffraction pattern of: (a) PLZT grain and (b) neighbouring grain of Pt lower electrode. Note on (a) the diffuse ring corresponding to d_{101} PLZT interreticular distance.

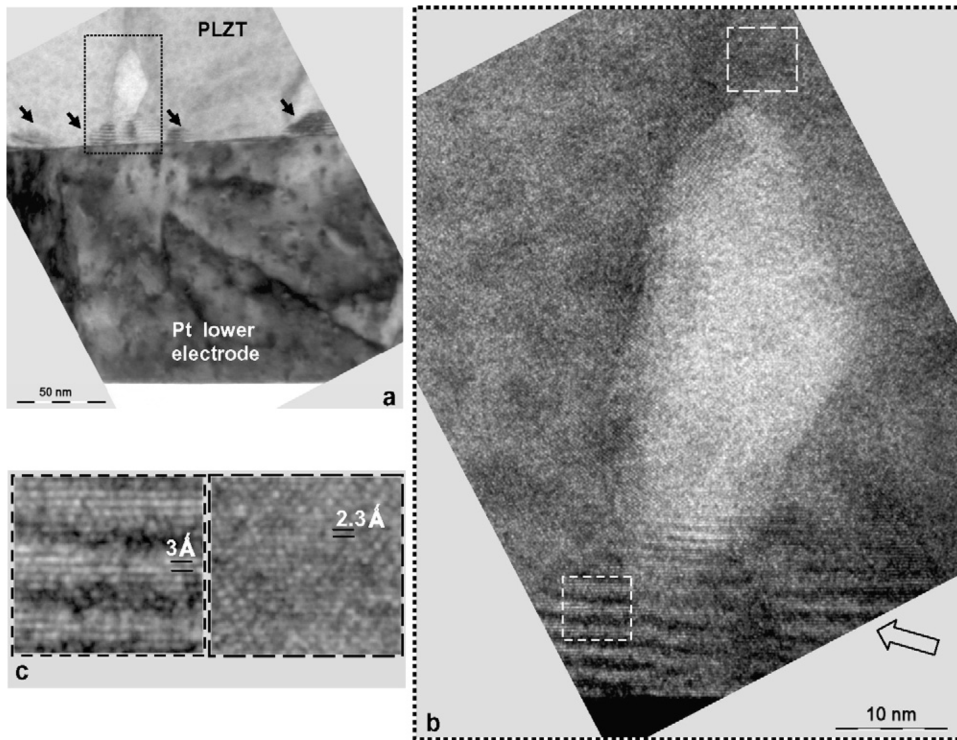

Fig. 7. TEM images of PLZT-Pt lower electrode interface.

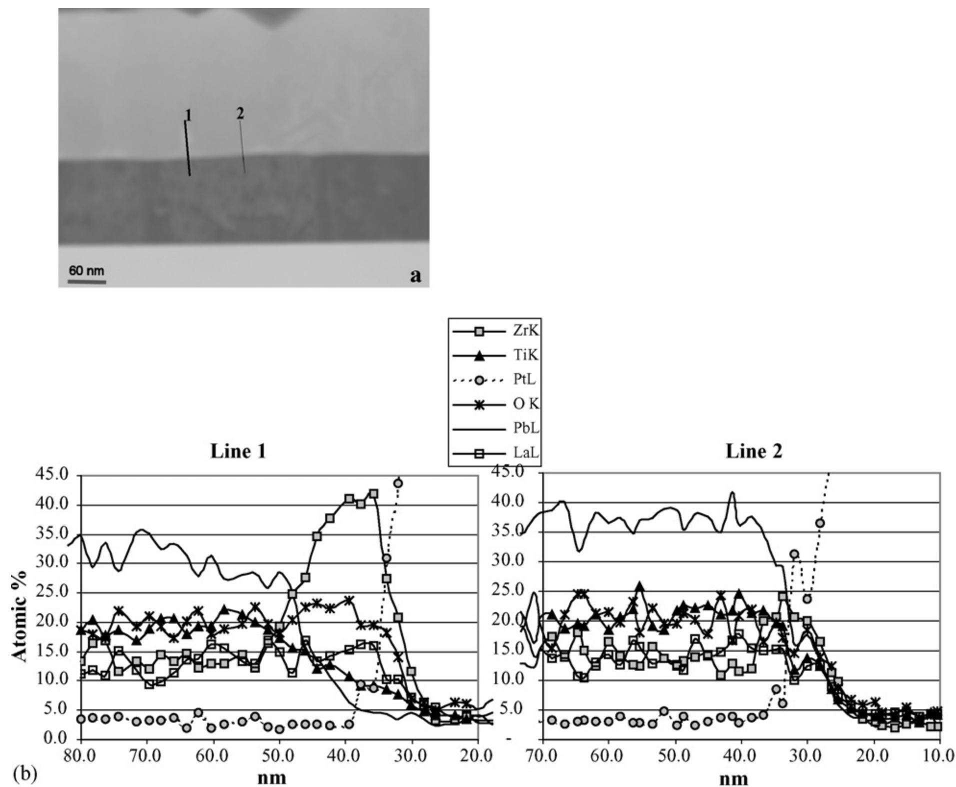

Fig. 8. (a) STEM image showing both lines followed with electron nanobeam for EDX line profiles; each measurement point is spaced of about 1.9 nm (b) partial corresponding EDX spectra; to ease interpretation both scales are expanded.

The width of the grains, ranging from 120 nm to 200 nm allowed performing micro-diffraction experiments. The textured nature of the PLZT film, was confirmed with $\langle 1\ 1\ 1\rangle_{PLZT}//\langle 1\ 1\ 1\rangle_{Pt}$ and perpendicular to growth plane. Besides, some micro-diffractions might exhibit diffuse rings corresponding to d_{110} (Fig. 6) suggesting the presence of small grains $\langle 1\ 0\ 1\rangle_{PLZT}$ oriented, which is in agreement with X-ray diffractograms (Fig. 2). High resolution observations and EDX analyses have brought further information on the microstructure of the film (Figs. 7 and 8), and especially on the first deposited atomic layers. Indeed, contrasts observed near the Pt–PLZT film interface suggest the presence of small grains, leading when superimposed to Moiré patterns (Fig. 7a and b). High resolution images of such a grain show fringes, spaced of 3 Å, which does not correspond to any PLZT structure interreticular distance (Fig. 7c). Also, a small grain showing a much clearer contrast than that of PLZT film can be distinguished.

Thus EDX line profiles have been performed in an attempt to identify those peculiar grains (Fig. 8). On the first one, the electron beam is shifted from Pt electrode to PLZT film going through ‘‘stranger’’ grains (Fig. 8b). For comparison, a second one is performed through the expected interface. In order to minimize superimposition effects, EDX analyses have been performed with a small tilt angle, explaining the unexpected low oxygen content. It clearly appears that the 3 Å characterized grain mainly contains Zr and La, it could thus be identified as $Zr_{0.9}La_{0.1}O_{1.95}$ phase, for which d_{101} = 2.99 Å. Also the clearer contrast grain seems to contain less Pb than the homogeneous PLZT film.

From these TEM observations, it is possible to conclude that a disturbed interfacial layer of around 10 nm exists at the interface between the PLZT film and the bottom electrode. In particular, some very small grains of $Zr_{0.9}La_{0.1}O_{1.95}$ were identified by EDX analysis. Then the classical reaction (1) between TiO_2 and PbO is certainly not the only mechanism that takes place at the first stage of the growth of our PLZT thin films. The interesting point in comparison with previous works is that an interfacial layer, different in nature from the ‘‘bulk layer’’, has been identified near the bottom electrode.

3.2. Thickness dependence of the electrical properties

Evolution of the structural and electrical properties of (1 1 1)-oriented films with thickness ranging from 50 nm to 650 nm has been examined. The diffraction patterns of the different films (Fig. 9a) show a gradual improvement of the degree of orientation of the film with the increase of their thickness. Indeed, the intensity of the (1 1 1) line increases with thickness, when the intensity of the (1 0 1) line tends to saturate (see Fig. 9b). This suggests that (1 0 1) orientation may arise from only few crystallites.

Hysteresis loops of the films show an improvement of the ferroelectric properties as the thickness is increased (Fig. 10a). It has to be noticed than the thinnest films, with thickness less than 135 nm, were too leaky to give a ferroelectric response, probably due to the columnar structure ‘‘defects’’. Well established loops with conventional shape were observed only for thickness of 135 nm and above. The average remanent polarization P_r and the average coercive field E_c for the film with a thickness of 270 nm were 12 $\mu C/cm^2$ and 45 kV/cm, respectively. The remanent polarization of the thicker film was improved reaching a value of 18 $\mu C/cm^2$, however with no significant variation of the coercive field, and of the polarization maximum. Fig. 10b shows permittivity and dielectric loss dependence on film thickness.

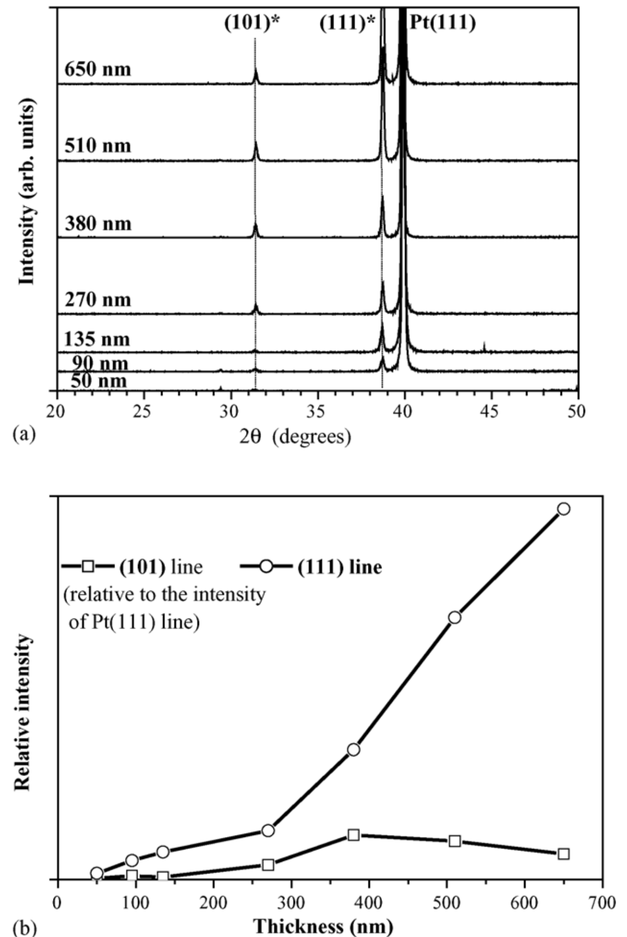

Fig. 9. (a) XRD patterns of PLZT films with thickness ranging from 50 nm to 650 nm. (b) Evolution with thickness of the relative intensities of (1 0 1) and (1 1 1) lines.

The thickness dependence of the electrical properties of our PLZT films are very similar to that observed in previous works [22–27]. Most of these works referred to the existence of a non ferroelectric dielectric layer at the electrode/film interfaces and it is probable that the Pt/film interfaces play a key role on the properties of our Pt/PLZT/Pt structures. Our TEM observations confirmed structural differences between a thin interfacial layer near the bottom electrode and the main film structure. Then, as demonstrated by Larsen et al. [22], Pt/PZT/Pt capacitors may be described by a linear interface capacitance in series with the linear capacitance due to the bulk ferroelectric layer. By assuming that the interface capacitance is independent of the

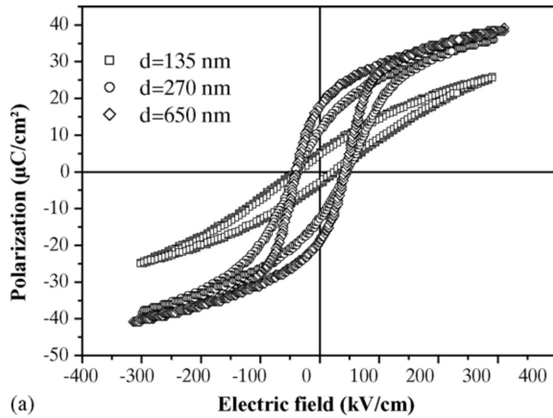

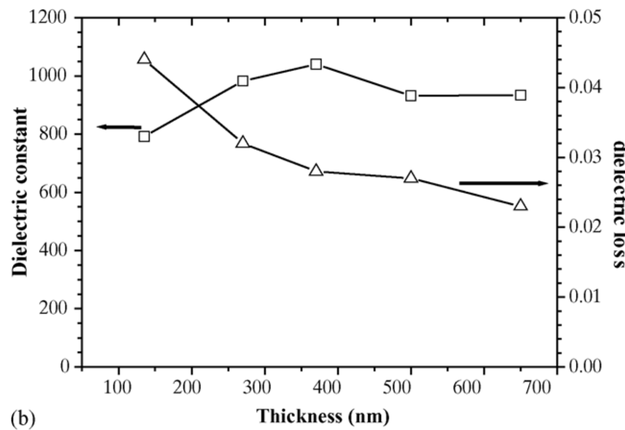

Fig. 10. Hysteresis loops of the samples with thickness of 135 nm, 270 nm and 650 nm. Evolution of the dielectric constant and loss with thickness of the films.

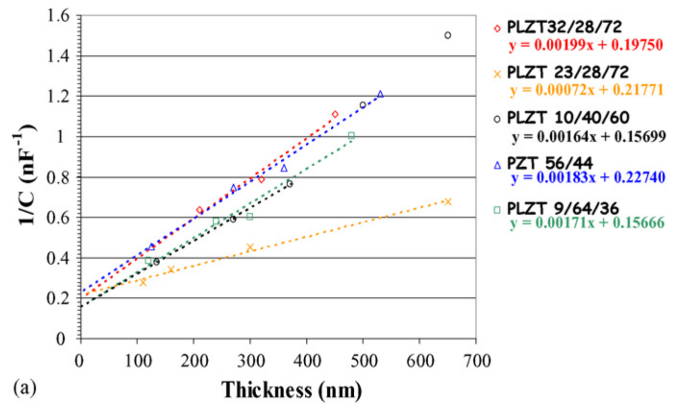

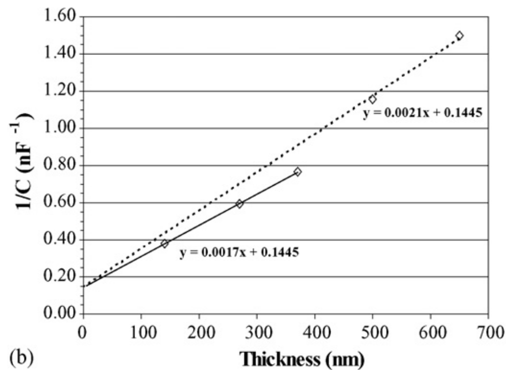

Fig. 11. Evolution of the reciprocal capacitance with thickness for different PLZT compositions. Evolution of the reciprocal capacitance with thickness for the PLZT 10/40/60.

film thickness, the total capacitance of the structure may be expressed as follows:

$$\frac{1}{C}=\frac{1}{C_{\mathrm{i}}}+\frac{d}{(\varepsilon_0\varepsilon_{\mathrm{r}}A)} \qquad (2)$$

where C is the measured capacitance, C_{i} the interface capacitance, d the total thickness of the sample, ε_0 and ε_{r} are the permittivity of free space and the relative permittivity of the film respectively, A the electrode area. It has to be noticed that relation (2) supposes that the thickness of the interface layers is negligible compared to that of the samples. This was confirmed by our TEM observations, from which an interfacial layer thickness of around 10 nm was estimated. The model was confirmed experimentally as it correctly predicted the observed linear variations of the reciprocal capacitance of PZT films versus their thickness [22]. Moreover, the determination of the interface capacitance and the dielectric permittivity of the bulk ferroelectric layer are possible. Different thickness series of samples with various compositions confirm the model (Fig. 11a). The calculated interfacial capacitances are found to be almost independant of the composition. The average calculated value, closed to 5.5 nF (see Table 1), is in agreement with previous results [22–24], even in case of Pt/$BaTiO_3$/Pt structure [25]. Nevertheless, the PLZT 10/40/60 needs the use of a specific interpretation to reach a same interfacial capacitance.

The plot of $1/C$ of this sample as a function of d is shown on Fig. 11b. The plot does not form a straight line. However it is possible to construct two different straight lines with different slopes but having same intercept with the Y-axis (see Fig. 11b). Both lines give an interface capacitance Ci of 6.9 nF, in agreement with the value found previously. Concerning the dielectric constant ε_{r} of the bulk ferroelectric layer, the latter may be determined from the slope of the curves, as suggested by relation (2). We found $\varepsilon_{\mathrm{r}} = 1200$ and $\varepsilon_{\mathrm{r}} = 980$ for the thinnest and for the thickest films, respectively.

The growth of all the films was performed under the same sputtering conditions. Thus, the different films presented

Table 1
Calculated values of interfacial capacitance and dielectric constant of the different series of PLZT samples

	PLZT 32/28/72	PLZT 23/28/72	PLZT 10/40/60	PLZT 0/54/46	PLZT 9/64/36
Calculated interfacial capacitance (nF)	5.1	4.6	6.9	4.4	6.4
Dielectric constant	1030	2840	1200	1120	1200

certainly similar interface quality, which justifies the use of an unique C_i value. It is interesting to note that the range of thickness (400–650 nm) for which is observed the change of ε_r value corresponds approximately to that for which was observed the saturation of the intensity of the (1 0 1) line (see Fig. 9b). Therefore one may conclude that the (1 0 1) oriented grains or/and the $Zr_{0.9}La_{0.1}O_{1.95}$ grains, even in a small amount, played a role on the average dielectric and ferroelectric properties of these PLZT films, though they were highly (1 1 1) oriented.

The measurement above showed that the contribution of the (1 0 1) oriented grains was to increase the overall dielectric constant since higher ε_r was found for the thinnest films for which larger volume fraction of (1 0 1) oriented grains was observed during the XRD measurements. But this is contradictory with some previous works showing that the dielectric constant of ⟨1 0 1⟩ oriented PZT films are lower than that of ⟨1 1 1⟩ oriented ones [28]. Therefore, it is possible that contribution of (1 1 1)/(1 0 1) grain boundaries may partly explain the increase of the dielectric response. Another hypothesis is to consider that the $Zr_{0.9}La_{0.1}O_{1.95}$ grains can also act as a dielectric dead layer. To obtain the right interface capacitance, the dielectric permittivity of the $Zr_{0.9}La_{0.1}O_{1.95}$ phase should be about 100, taking into account the thickness of the dead layer as determined by TEM observations.

Another possible contribution for the observed dependence of ε_r value on film thickness could result from some relaxation of the strain imposed by the lattice mismatch between the film and the substrate. Though the latter was found not to be excessive (2.5%), the strain effects might however influence the dielectric and ferroelectric properties of the films with thickness below 300–400 nm, and thicker films should experience the effect of the strain relaxation.

4. Conclusion

(1 1 1)-oriented PLZT thin films grown by sputtering on Si/Pt substrates have been investigated. The effect of the thickness of ultra thin seeding layer on in situ crystallization was demonstrated. By this way, in situ crystallisation at moderate temperatures was possible, even for oriented films. The PLZT thin films displayed good dielectric properties which highlights their promising potential for DRAM applications. However detrimental effect of electrode/film interfaces must be taken into consideration as they play a key role on the dielectric and ferroelectric properties when the thickness of Pt/PLZT film/Pt capacitors is reduced. TEM observations have evidenced that an interfacial layer containing very small grains of $Zr_{0.9}La_{0.1}O_{1.95}$ exists for the films studied in this paper.

Acknowledgments

The authors would like to thank Dr. Manaud, Dr. Lahaye and Dr. Maglione from ICMCB laboratory of Bordeaux for A.E.S depth profile analysis. This work was supported by the Centre National de Recherche Technologique Matériaux de Basse-Normandie and also the ‘‘Region of Basse-Normandie’’.

References

[1] J.F. Scott, C.A. Araujo, Science 246 (1989) 1400.
[2] C.H. Ahn, K.M. Rabe, J.-M. Triscone, Science 303 (2004) 488.
[3] Q. Tan, Z. Xu, J.-F. Li, D. Viehland, Appl. Phys. Lett. 71 (1997) 1062.
[4] W.S. Kim, S. Ha, H.-H. Park, C.E. Kim, Thin Solid Films 355 (1999) 531.
[5] H.-H. Ho, H.-H. Park, R.H. Hill, Appl. Surf. Sci. 237 (2004) 427.
[6] X. Dai, A. DiGiovanni, D. Viehland, J. Appl. Phys. 74 (1993) 3399.
[7] G.H. Haertling, C.E. Land, J. Am. Ceram. Soc. 54 (1971) 1.
[8] M.E. Lines, A.M. Glass, Principles and Applications of Ferroelectric and Related Materials, Oxford Science Publications.
[9] H. Roberts, B. Otterloo, EFUG2001, Arcachon.
[10] R. Bouregba, G. Poullain, B. Vilquin, H Murray, Mater. Res. Bull. 35 (2000) 1381.
[11] P. Muralt, T. Maeder, L. Sagalowicz, S. Hiboux, S. Scalese, D. Naumovic, R.G. Agostino, N. Xantopoulos, H.-J. Mathieu, L. Patthey, E.L. Bullock, J. Appl. Phys. 83 (1998) 3835.
[12] S. Hiboux, P. Muralt, J. Eur. Ceram. Soc. 24 (2004) 1593.
[13] M.L. Calzada, R. Poyato, J. Garcia Lopez, M.A. Respaldiza, J. Ricote, L. Pardo, J. Eur. Ceram. Soc. 21 (2001) 1529.
[14] B. Vilquin, R. Bouregba, G. Poullain, M. Hervieu, H. Murray, Eur. Phys. J. AP 15 (2001) 153.
[15] H.-H. Kim, S.-T. Kim, W.-J. Lee, Thin Solid Films 324 (1998) 101.
[16] W. Gong, J.-F. Li, X. Chu, Z. Gui, L. Li, J. Appl. Phys. 96 (2004) 590.
[17] G. Vélu, B. Jaber, T. Haccart, D. Remiens, J. Phys. IV (France) 8 (1998) 243.
[18] Z. Huang, Q. Zang, R.W. Whatmore, J. Appl. Phys. 85 (1999) 7355.
[19] X.G. Tang, A.L. Ding, Y. Ye, W.X. Chen, Thin Solid Films 423 (1999) 13.
[20] K. Aoki, Y. Fukuda, K. Numata, A. Nishimura, Jpn. J. Appl. Phys. 34 (1995) 192.
[21] K. Wasa, Revista Brasileira de Aplicaçoes de Vacuoe 20 (2001).
[22] P.K. Larsen, G.J.M. Dormans, D.J. Taylor, P.J. van Veldhoven, J. Appl. Phys. 76 (1994) 2405.
[23] G. Le Rhun, Ph.D. dissertation, University of Caen, France, 2004.
[24] S.-H. Lee, H.-J. Joo, J.-P. Kim, J.-H. Jung, M.-K. Ryu, S.-S. Lee, M.-S. Jang, S. Yi, J. Korean Phys. Soc. 35 (1999) S1172.
[25] Y.W. Cho, S.K. Choi, G. Venkata Rao, Appl. Phys. Lett. 86 (2005) 202905.
[26] G. Vélu, D. Remiens, Microelectron. Reliability 39 (1999) 241.
[27] K.R. Udayakumar, P.J. Schuele, J. Chen, S.B. Krupanidhi, L.E. Cross, J. Appl. Phys. 77 (1994) 3981.
[28] S. Yokoyama, Y. Honda, H. Morioka, S. Okamoto, H. Funakubo, T. Iijima, H. Matsuda, K. Saito, T. Yamamoto, H. Okino, O. Sakata, S. Kimura, J. Appl. Phys. 98 (2005) 094106.